Perspective

Scanning transmission electron microscopy for advanced characterization of ferroic materials

Matthew J. Cabral[1,3] iD **, Zibin Chen**[2] iD **, Xiaozhou Liao**[3] iD

[1]Department of Chemical Engineering, University of Rhode Island, Kingston, RI 02881, USA.
[2]Department of Industrial and Systems Engineering, Research Institute for Advanced Manufacturing, The Hong Kong Polytechnic University, Hong Kong, China.
[3]School of Aerospace, Mechanical and Mechatronic Engineering, The University of Sydney, Sydney, NSW 2006, Australia.

Correspondence to: Dr. Matthew J. Cabral, Department of Chemical Engineering, University of Rhode Island, 2 East Alumni Ave Room 084, Kingston, RI 02881, USA. E-mail: matthew.cabral@uri.edu

Abstract

Scanning Transmission electron microscopy (STEM) technologies have undergone significant advancements in the last two decades. Advancements in aberration-correction technology, ultra-high energy resolution monochromators, and state-of-the-art detectors/cameras have established STEM as an essential tool for investigating material chemistry and structure from the micro to the atomic scale. This characterization technique has been invaluable for understanding and characterizing the origins of ferroic material properties in next-generation advanced materials. Many unique properties of engineering materials, such as ferroelectricity, piezoelectricity, and ferromagnetism, are intricately linked to their atomic-scale composition and structure. STEM enables direct observation of these structural characteristics, establishing a link with macroscopic properties. In this perspective, we provide an overview of the application of advanced STEM techniques in investigating the origin of ferroic material properties, along with discussions on potential opportunities for further utilization of STEM techniques.

Keywords: Scanning transmission electron microscopy, materials characterization, ferroic materials, aberration-correction, image analysis, atomic resolution imaging

INTRODUCTION

Ferroic materials constitute a crucial category of materials that possess a variety of unique properties, including ferroelectricity, ferromagnetism, and ferroelasticity, that are employed in numerous applications. These applications encompass areas such as energy harvesting, sensors, medical imaging, and consumer electronics[1-5]. The properties and performance of these materials are intricately linked to their atomic-scale structures and chemistries. In certain instances, even a slight modification in composition can profoundly influence material performance. For instance, in both ceramics and single crystals, the piezoelectric coefficient of the relaxor ferroelectric PMN-PT can be nearly doubled by substituting < 1 mol% samarium (Sm) for lead (Pb) as demonstrated by Li *et al.*[6,7]. Additionally, incorporating elements with varying valence states, ionic radii, electronegativities, and polarizabilities holds great potential in bolstering the piezoelectric and dielectric characteristics of ferroic materials, as demonstrated in the case of high-entropy alloys[8]. Understanding the correlation between chemical distribution and structure becomes pivotal in comprehending the enhanced piezoelectric properties that arise in these materials. This understanding can be harnessed to design and engineer the next generation of high-performance ferroic materials.

Advanced scanning transmission electron microscopy (STEM) is an exceptionally powerful tool that enables direct visualization of atomic structure and chemistry in numerous materials. While electron microscopes have long provided nanometer-scale resolutions, the introduction of aberration-correction technology at the beginning of the 21st century has pushed the limits of resolution to sub-Angstrom length scales[9-11]. This significant enhancement in imaging resolution, combined with improved accuracy and precision in STEM imaging, has ushered in a new era of electron microscopy applications. By harnessing the capabilities of an Angstrom-sized probe, it becomes possible to directly visualize atomic-scale chemistry and structure. For instance, annular dark-field (ADF) STEM imaging employs the mass contrast (Z) provided by the technique to identify individual dopant atoms within a bulk material[12,13]. These techniques have further advanced, with electron ptychography achieving reported STEM resolutions as fine as 39 pm and capable of resolving interstitial atoms in a matrix[14,15]. Moreover, imaging techniques in electron microscopes can readily integrate with spectroscopic methods, such as energy-dispersive X-ray spectroscopy (EDS) and electron energy loss spectroscopy (EELS), facilitating the examination of atomic-scale chemistry, electronic structure, and even vibrational modes[16,17].

STEM continues to be a vital tool for studies of ferroic and other functional materials. These applications will continue to evolve with developments in electron optics, instrumentation, detectors, and *in-situ* capabilities[18]. Techniques, such as electron ptychography[14], 4D-STEM[19], and ultra-high energy resolution EELS[17], have allowed for the characterization of parameters, such as polarization, chemical/structural ordering, oxidation states, and electronic structure, at sub-nanometer length scales. Despite the technological advancements, increased accessibility, and user-friendliness of electron microscopes, which are now widely available in both industry and academia, a key challenge remains in bridging the gap between researchers specializing in electron microscopy technique development and materials researchers. Nonetheless, it is crucial for scientists in both domains to recognize the broad applicability of STEM for characterizing multifunctional materials. This perspective aims to provide insights into the latest developments in STEM instrumentation and techniques, emphasizing their broad utilization in ferroic materials research. Additionally, opportunities for in-depth data analysis to address materials-related questions will be discussed.

Basics of S/TEM

Aberration-correction technology has advanced the resolving power of conventional TEM and STEM from the nanometer to sub-Angstrom scales. High-resolution TEM (HRTEM) and STEM differ in electron optics

and image formation. HRTEM [Figure 1A] employs a broad, parallel electron beam that results in a coherent image that is affected by sample thickness and objective lens defocus. Interpreting HRTEM images requires image simulations to understand the impact of thickness and defocus on the resulting image[20,21]. Conversely, STEM [Figure 1B], including a scanning electron microscope (SEM), uses a finely focused electron probe scanned pixel by pixel with electrons scattering in all directions. STEM imaging can be performed with conventional detectors or by using pixelated detectors for 4D-STEM [Figure 1C], which will be discussed in later sections. With higher voltages and aberration-correction, STEM significantly enhances resolving power. Compared to HRTEM, the incoherent image formation of STEM yields a contrast that is proportional to both atomic number and sample thickness. These directly interpretable images reveal atomic column positions and intensities corresponding to crystallographic locations and atomic numbers.

Atomic resolution imaging

Engineering ferroic materials involves multiple considerations. By manipulating chemistry at the atomic level, mixed phases, defect structures, and interfaces can be formed, significantly impacting material properties. STEM imaging is a valuable technique for directly observing these features and providing essential information. ADF imaging is commonly associated with STEM imaging. As a finely focused probe scans the sample, electrons undergo various forms of scattering during transmission. Rutherford scattering, characterized by elastic scattering due to Coulomb interaction, results in large-angle scattering (> 50 mrad), producing atom column intensities proportional to $\sim Z^{1.7}$ and sample thickness referred to as high-angle ADF (HAADF) imaging[22,23]. By modifying the inner collection angle of a detector, such as to 25 mrad, the resulting image is low-angle ADF (LAADF) imaging, revealing strain contrast from inelastically scattered electrons[24]. Figure 2A demonstrates the contrast variations between HAADF [Figure 2A(a)] and LAADF [Figure 2A(b and c)] STEM by modifying the detector inner collection angle for a low-angle twist grain boundary at a $SrTiO_3/Nb:SrTiO_3$ interface[25]. Consequently, ADF-STEM allows for precise atomic column localization, contrast reflecting strain effects, and atom column contrast proportional to the chemical composition of the imaged structure based on the inner semi-angle of the detector.

With its sub-Angstrom spatial resolution and strong correlation between atomic number and contrast, HAADF-STEM is highly valuable for examining structures, characterizing interfaces, and studying defect structures in various piezoelectric materials. For instance, it is an effective tool for investigating chemical and structural order in materials, including A- and B-site ordered double perovskites such as $NaLaMgWO_6$ ceramics. These materials exhibit layered A-site ordering and B-site rock-salt ordering, which is attributed to a large energy barrier that results in non-switchable ferroelectric polarization[26]. Using HAADF-STEM, this double perovskite structured ordered ceramic can be characterized by its structure and chemical distributions along various zone axes, as shown in Figure 2B. Cation ordering can be observed along the [111], [110], and [100] orientations by experiment [Figure 2B(a-c)] and confirmed by image simulation of the same orientations [Figure 2B(d-f)]. Although the cation ordering can be seen clearly due to the differences in Z-contrast of the constituent elements, the observations can be further confirmed by atomic resolution EDS mapping [Figure 2B(g-i)][26]. In addition to providing clear insights into chemical order, HAADF-STEM is also useful for quantifying polarization in ferroic materials. The positions of atomic columns can be utilized to quantify polarization in layered structures [Figure 2C], such as thin films of the multiferroic $BiFiO_3$ with varying doping profiles[27]. These displacements can either be plotted directly on the ADF-STEM image [Figure 2C(a)] or averaged and plotted separately on a line-by-line basis [Figure 2C(b)]. These studies are particularly significant due to the emerging nature of these materials and the need to optimize their performance by structural modification for widespread applications.
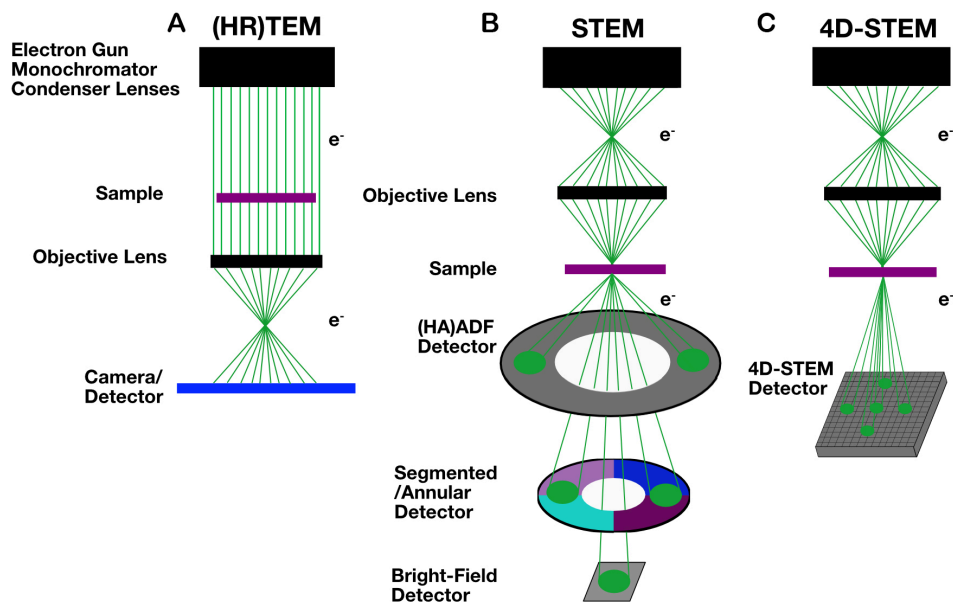
Figure 1. Schematic overview of (A) (HR)TEM, (B) STEM, and (C) 4D-STEM in electron microscopes.

Imaging atomic columns of light elements

Characterizing light elements is crucial in ferroic materials because their properties are often linked to the displacement of cations relative to anions. Elements such as oxygen (Z = 8) and lighter are typically described as light elements and generally occupy anion sites in ferroic materials. Moreover, materials may contain cations, anions, or dopants, such as H, O, N, or Li, or have light elements occupying cation sites, as seen in $LiNbO_3$, a ferroelectric material widely used in non-linear optics and acoustic devices[28]. Additional consideration should also be given to the difference between Z of the different elements. For example, in PMN-PT, there is a large difference in atomic numbers between Pb (Z = 82) and Mg (Z = 12), which can make it difficult to visualize Mg-rich atomic columns. HAADF-STEM, being strongly proportional to atomic number (Z), tends to emphasize heavier elements, making visualization of lighter elements challenging. To enhance the contrast of lighter elements, the collection angle of the annular detector can be reduced, as done in bright-field (BF) and annular BF (ABF) STEM imaging. BF-STEM uses a detector collection angle of approximately 0-20 mrad, while ABF-STEM collects scattered electrons in the range of 10-20 mrad[29-31]. By narrowing the inner collection angle range in BF-STEM and ABF-STEM, the resulting images rely more on phase contrast rather than mass contrast, making them more sensitive to elements as light as hydrogen[32]. Modern scanning/transmission electron microscopy (S/TEMs) are equipped with multiple annular detectors, enabling simultaneous collection of signals for BF, ABF, and ADF-STEM imaging. This simultaneous imaging capability has facilitated the observation of light elements, such as the oxygen anion in $SrTiO_3$, as shown in Figure 3A[33]. However, there are limitations to BF and ABF-STEM, including the requirement for ultrathin samples, a poor signal-to-noise ratio, a strong dependence on defocus, and the need for careful microscope alignment[20].

An alternative to BF and ABF STEM image modes for imaging light elements is integrated differential phase contrast (iDPC) imaging, which utilizes a segmented ADF detector. This technique is an extension of differential phase contrast (DPC) imaging, initially introduced in the 1970s for imaging ferromagnetic samples by measuring changes in the center of mass (COM) of electron beams caused by the electric potential of samples[18,36-38]. DPC proves particularly valuable for ferroelectric materials such as $Pb(Zr_{0.2}Ti_{0.8})O_3$ thin films, where the polar distortion of Ti cations results in visible contrast variations [Figure 3B]
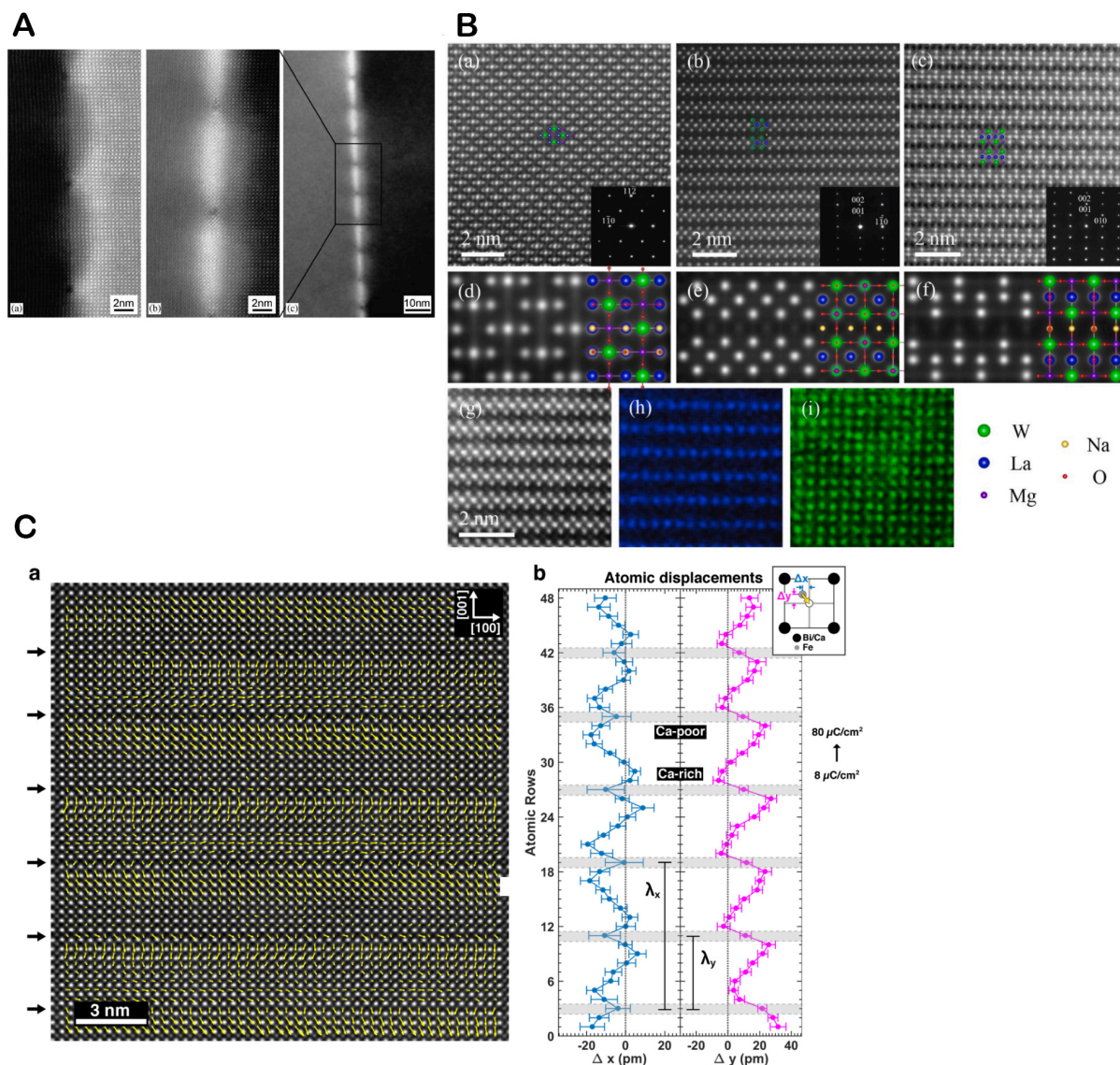
Figure 2. (A) HAADF-STEM (a) and LAADF-STEM (b and c) of a low-angle twist grain boundary between $SrTiO_3$ and Nb: $SrTiO_3$, demonstrating the effect of crystal orientation and strain fields for the respective imaging conditions. Reprinted with permission[25]. Copyright © 2007 Elsevier. (B) HAADF-STEM images of $NaLaMgWO_6$ ceramics taken along the [111], [110], and [100] zone axes (a-c) confirmed by STEM image simulations for each zone (d-f). Chemical order further confirmed by atomic resolution EDS mapping (g-i). Reprinted with permission[26]. Copyright © 2022 Elsevier. (C) Polarization map superimposed on HAADF-STEM image of Ca-doped $BiFeO_3$ thin films. Profiles of in-plane and out-of-plane displacement components are also displayed. Reprinted with permission[27]. Copyright © 2018 American Chemical Society.

between ferroelectric domains[34]. More recently, DPC has been implemented for atomic resolution STEM imaging using an ADF detector with between 2-16 segments. A 4-quadrant detector is commonly utilized where an acquired two-component vector image (DPC_x = a-c and DPC_y = b-d) is subjected to 2D integration with the segmented detector, resulting in the iDPC image[35,39]. Figure 3C showcases instances of iDPC imaging in gallium nitride (GaN) oriented along the [11$\bar{2}$0] and [10$\bar{1}$1] orientations, illustrating the remarkable resolving power of this technique[35]. This imaging mode is sensitive to both light and heavy elements, less sensitive to defocus, and exhibits higher signal-to-noise ratios compared to other techniques for imaging light elements. However, iDPC requires extremely thin, flat, and contamination-free samples
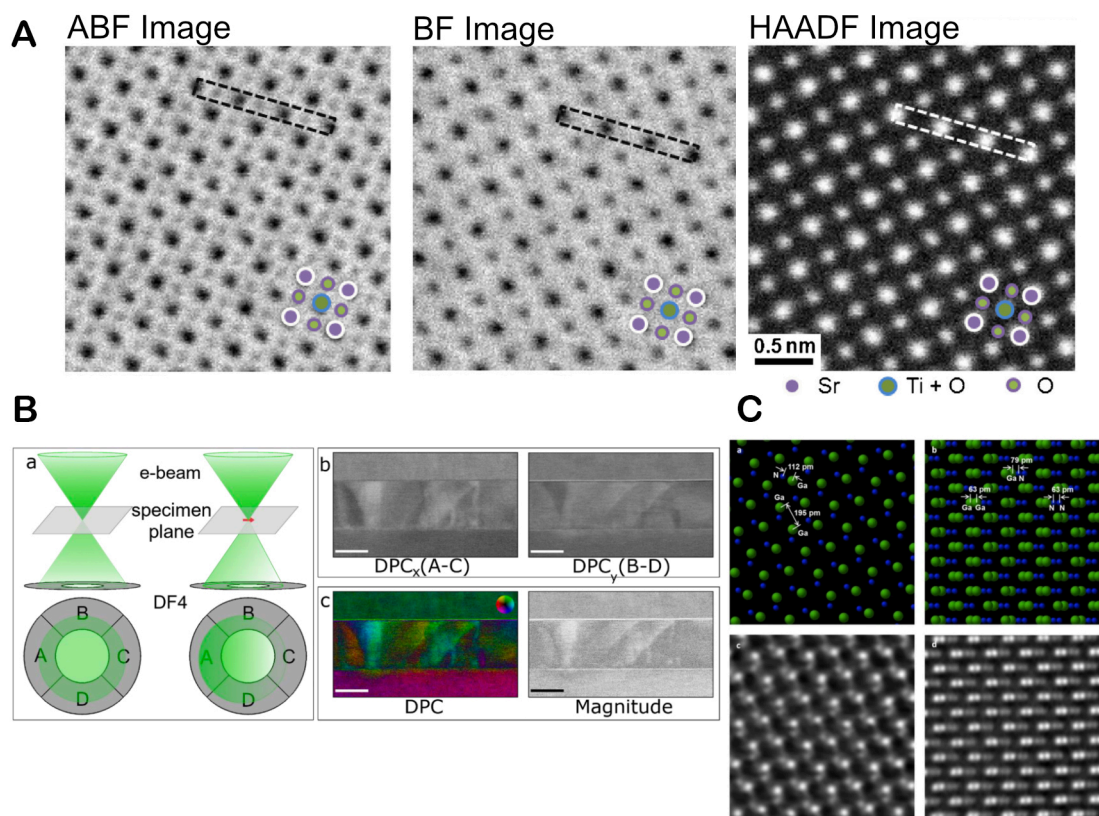
Figure 3. (A) Atomic resolution images of $SrTiO_3$ viewed along the [001] direction with ABF (11-22 mrad), BF (0-22 mrad), and ADF (90-170 mrad) STEM images. Adapted with permission[33]. Copyright © 2012 Elsevier. (B) DPC detector configuration with accompanying A-C and B-D STEM images of the ferroelectric $Pb(Zr_{0.2}Ti_{0.8})O_3$ thin films. Contrast resulting from the ferroelectric domain structures in $Pb(Zr_{0.2}Ti_{0.8})O_3$ are visible. Reprinted with permission[34] Copyright © 2021 MDPI. (C) Atomic resolution iDPC images of gallium nitride (GaN) oriented along the [11$\bar{2}$0] and [10$\bar{1}$1] orientations. Reprinted with permission[35]. Copyright © 2018 Nature Publishing Group.

carefully tilted on a zone axis for optimal imaging[20]. Despite the challenges involved in imaging light elements, the ability to do so simultaneously with other imaging modes, such as ADF imaging, offers a powerful method for characterizing atomic structures and chemistry at the atomic scale. For instance, simultaneous ADF and iDPC imaging were employed to investigate the atomic structure of the relaxor ferroelectric PMN-PT with varying Ti content. This allowed for a direct correlation of local chemistry with polarization, octahedral distortion, and octahedral tilting[40]. These observations are crucial for understanding the origin of relaxor ferroelectricity and providing insights into how local structures can be engineered to optimize material properties.

Direct electron detectors and four-dimensional STEM

In the last decade, four-dimensional STEM (4D-STEM) has attracted significant research interest, given its plentiful prospects for material analysis. Conventional STEM detector technology converts the electrons collected at each pixel into a single value representing the contrast. While this number can be expanded upon by using segmented detectors, 4D-STEM refers to the recording of 2D images of the electron probe at each pixel in a 2D image, as illustrated in Figure 1C[19,41,42]. Although there are numerous detector configurations that can be utilized for the collection of 4D-STEM, one of the most widely available detectors is the electron microscope pixel array detector (EMPAD), which is manufactured by Thermofisher Scientific. The EMPAD is composed of a collection of photodiodes arranged on an integrated circuit that

collects electrons at each pixel position, converting them to a charge pulse. This charge pulse is integrated over time to produce a signal that is directly proportional to the number of electrons collected. This configuration results in a detection system that is sensitive to a single electron and yields a dynamic range of 1,000,000:1 with fast readout speeds[19,43,44]. Although the number of pixels (128 × 128) in the EMPAD is comparatively small, collecting diffraction at each probe position enables extensive opportunities for analysis, including crystallographic orientation measurements, strain mapping, phase mapping, and other diffraction-based analyses. Moreover, the collection of the total electron diffraction pattern allows for the use of "virtual detectors", which can be used to reconstruct any imaging mode, including HAADF, BF, DPC, *etc.*, through post processing.

Direct electron and pixelated detectors have enabled the development of advanced techniques such as electron ptychography. Although the resolution of conventional STEM imaging is limited by diffraction and the optics of the microscope, electron ptychography presents a way of overcoming these limits. By using a high-speed pixelated detector or direct electron detector that is sensitive to single electrons, the interference patterns of the scattered beams can be resolved and analyzed to determine the phase of the object. These patterns can then be used to reconstruct the image through post processing, thereby overcoming conventional diffraction limitations[14,45]. Electron ptychography is a rapidly advancing technique that holds great promise due to its numerous applications, including applicability for biological imaging, imaging beam-sensitive materials, characterizing magnetic materials, and measuring strain in materials at sub-Angstrom length scales[46,47].

Four-dimensional STEM presents numerous opportunities for advanced characterization of ferroic and other functional materials. The combined real space image with a corresponding diffraction pattern opens the opportunity to measure strain at material interfaces at atomic resolution by analyzing the distances between the diffraction disks[48,49]. Further, diffraction patterns can be analyzed at each pixel in a 4D-STEM dataset to identify order/disorder nanostructures in ferroic materials. Nanobeam diffraction is highly sensitive to subtle changes in microstructure, enabling the identification of rhombohedral nanostructures in the tetragonal and orthorhombic phases of $BaTiO_3$[50]. This study demonstrates the unique ability for local diffraction observations in an otherwise average technique as for neutron and x-ray diffraction. Four-dimensional STEM continues to see numerous applications, including many in piezoelectric and other functional materials, but data analysis remains a critical step to obtaining useful information.

In-situ S/TEM

The structure, chemical distribution, and properties of ferroic materials, including ferroelectricity and ferromagnetism, are strongly linked to external stimuli such as temperature, electrical biasing, and strain. Understanding how ferroic materials respond to these stimuli is critical for understanding the fundamental mechanisms that result in their properties, including domain switching kinetics, domain growth, and phase transitions[51]. To this end, the evolution of *in-situ* electron microscopy technology provides an extensive opportunity to study the dynamic processes of ferroic materials. While *in-situ* capabilities have been available in electron microscopes for decades, they have been limited by factors such as sample drift due to environmental changes. The combined improved stability of S/TEMs with innovative *in-situ* holder technology now enables direct observation of materials kinetics at sub-Angstrom resolution[52].

The opportunities for *in-situ* S/TEMs are extensive and include liquid cell electron microscopy[53,54], heating[55,56], cooling[51,57], biasing[58,59], and mechanical stressing[60-62]. While behaviors, such as domain wall motion and domain switching, can be observed using conventional TEM, the emergence of sub-Angstrom resolution, combined ADF/iDPC imaging, and 4D-STEM offer the opportunity for more in-depth

characterization and analysis. Although in-depth details of these techniques are beyond the scope of this perspective, comprehensive reviews are available that outline ongoing and future research directions of *in-situ* S/TEM[63-65].

Analysis tools for electron microscopy data

With recent advancements in S/TEM instrumentation and technology, ease of use has increased dramatically. Many modern aberration-corrected microscopes are now equipped with software allowing for automatic tuning, greatly speeding up the process and ease of use for users. The coupled with improved microscope stability allows users to align the microscope and tune the corrector within a matter of minutes. Furthermore, many electron microscopes in shared user facilities are housed in carefully designed rooms that mitigate instabilities resulting from noise, temperature variations, mechanical vibrations, acoustical sources, and magnetic sources[66]. With all these advancements, high-quality data collection can be performed much more efficiently, allowing for more time to perform post processing. In the following sections, we will detail various software tools that allow the correction of distortion in electron microscopy data and simplified post processing.

Correcting drift and distortion in STEM images

Despite significant improvements in the spatial resolution and stability of electron microscopes, sample drift and scanning distortion remain challenges for achieving accuracy and precision in STEM data. These issues arise from both intrinsic scanning distortion caused by the movement of the electron probe across the sample and external sources of drift[67]. As a result, captured atomic resolution images may exhibit a combination of expansion, compression, and shearing, which hampers the accurate measurement of structural features such as lattice distances, atom column intensities, and polarization. Even the most stable microscopes can experience small quantities of drift over long acquisition times. To address these distortions, various techniques have been developed for correction in electron microscopy and other high spatial resolution techniques, such as scanning probe microscopy (SPM). One approach involves utilizing prior knowledge of the atomic features to correct distortions[68]. However, this information may not be available when studying novel materials. Another method involves using a known standard sample (e.g., Si or SrTiO$_3$) to measure drift and distortion, which can then be applied to the samples of interest[69]. In the case of beam-sensitive samples, a non-rigid image registration method can be employed using a series of images acquired at a low electron dose. This approach is particularly useful for noisy data, as it allows alignment of similar features from multiple images to a single image with a sufficient signal-to-noise ratio[70-72]. These techniques offer effective ways to address sample drift and scanning distortion, enabling more accurate characterization of materials at the atomic scale.

One of the most frequently used techniques to correct sample drift and distortion is capturing a series of images and recombining them during post-processing. Many electron microscope user interfaces have tools built in for this approach, such as drift-corrected frame integration (DCFI) on Thermo Fisher Scientific instruments[73], or they can be installed as plugins, such as those available for Digital Micrograph. However, although these tools are easy to use, they may not correct for non-linear drift and scan distortions. In such cases, other post-processing tools, including revolving STEM (RevSTEM), can be employed[74]. RevSTEM captures a series of images with a short time/pixel dwell time and a 90° scan rotation between subsequent frames. By rotating the scanning system between successive frames, sample drift and distortion can be quantified and corrected through post-processing[74]. Scanning distortion can also be corrected by quantifying it on a standard sample (such as Si or SrTiO$_3$) and mathematically applying it to the other images using an affine transformation. Another procedure for correcting non-linear drift distortion involves using orthogonal image pairs (90° rotation between images) to align the images by fitting contrast variations in the slow scan direction on a line-by-line basis[67]. Although only two images are necessary for this process,

additional orthogonal images can be included in the correction. By applying such programs, STEM images free of artifacts resulting from sample drift or scanning distortions can be obtained for further quantification.

Identifying positions of atomic columns

Material properties often result from complex relationships between chemical distribution and structural distortions that occur at the atomic scale. To gain a better understanding of how these phenomena emerge at the macroscale, it is crucial to comprehend the connection between atomic structure and material properties. STEM imaging offers a valuable means of investigating both structure and chemistry at the atomic scale with accuracy and precision. Thanks to advancements in instrumentation and the elimination of artifacts in atomic resolution images, it is now possible to directly make accurate and reproducible crystallographic measurements in real space[75]. In the following sections, we will introduce several tools that are available to extract and quantify useful information from atomic resolution images.

Before the widespread availability of aberration-corrected microscopes, advanced image analysis was mainly conducted by specialized electron microscopy research groups. Manual identification of thousands of atomic columns in atomic resolution images was a cumbersome and impractical process. As the technique became more popular, efforts focused on developing tools for rapid analysis of multiple images. Various approaches have been identified, including principal component analysis (PCA)[76] and template matching[77]. These techniques are particularly effective for detailed analysis of materials at length scales unattainable with other characterization methods. For example, in the case of a multiferroic $BiFeO_3$ thin film, initial guesses, followed by COM calculations, can determine the positions of cations and oxygen with PCA, which can then be applied to extract information on atomic column shape[76]. Combining this data with STEM image simulations[78-80] reveals octahedral tilting at domain walls, providing parameters applicable to theory. Such analyses are especially valuable for researchers investigating structure-property relationships in material design.

Numerous tools now facilitate rapid quantitative analysis of atomic resolution images. These tools include Atom Column Indexing (ACI)[81], Atomap[82], StatSTEM[83], CalAtom[84], and Oxygen octahedra picker[85]. Most of these programs offer freely available source code online and utilize popular engineering software, such as MATLAB or Python. Additionally, software plugins such as DMPFIT can be installed on Digital Micrograph for atom column fitting and analysis[86]. These programs employ various algorithms to identify and quantify atom column positions with sub-pixel precision. For example, ACI utilizes the image processing toolbox of MATLAB for normalized cross-correlation, Gaussian template matching, and 2D Gaussian fitting to determine column centers of mass, intensities, and shapes[81]. ACI projects atom column positions onto non-collinear reference vectors, assigning each column an (i, j) matrix index, facilitating lattice analysis and quantitative calculations. In perovskite-structured oxides, matrix indices of atomic columns allow direct comparison of nearest neighbor distances and intensities, providing insights into the relationship between chemical distribution and structural distortion[87]. Furthermore, direct analysis of atom-atom distances enables strain mapping over large areas, replacing conventional methods such as geometric phase analysis (GPA) or nanobeam electron diffraction[88-90].

One of the best opportunities arising from recent developments in advanced electron microscope imaging and analysis software is the detailed study of oxygen structure in piezoelectric materials with perovskite or spinel structures. Many outstanding properties, such as antiferroelectricity, relaxor ferroelectricity, and magnetoelectric properties, result from the interplay of polarization and chemical ordering, which are evident in the tilting/distortion of oxygen octahedra[76,91-94]. While BF and ABF-STEM have been widely

available for decades, the emergence of iDPC imaging provides an alternative means of imaging light elements with high contrast. Although these light element columns may be readily identifiable by visual inspection, difficulties may arise in extracting and segregating more than two atom column types, especially with a large contrast variation. Atomap, which is written in Python, is another freely available software package that facilitates the identification of multiple atom column types. Atomap has numerous advantages, including being programmed in Python, which is a free programming language (in contrast to MATLAB), has graphical user interface (GUI) functionality to assist with analysis, has well-developed documentation with examples, and is being expanded upon by other researchers to increase functionality. In common with many of the introduced programs, Atomap utilizes a model-based approach and 2D Gaussian fitting to first identify and locate the most intense atom column types. These intense columns can then be subtracted from the image, simplifying the process of extracting information from low-contrast sublattice sites[82]. Since multiple STEM imaging modes can be performed simultaneously, this provides the opportunity to identify cation atom column positions in a HAADF image and subtract them from a BF/ABF/iDPC image to extract oxygen positions. With this approach, multiple atom column sublattice types can be extracted for individual analysis or determining relationships between them.

Quantification of atomic resolution data

Typically, the most challenging aspect of extracting quantitative information from electron microscopy images is locating and identifying all the atomic columns and storing this information in a format that can be easily manipulated. For example, distances between similar columns can be investigated using a projected pair distribution function [Figure 4A], which is analogous to the PDF techniques utilized in diffraction[87]. In addition to locating atomic columns, Atomap offers numerous built-in functions that allow for a variety of analyses, such as measuring monolayer distances, calculating distances between different atom types [Figure 4B], drawing line profiles, determining polarization, and plotting pair distribution functions[82].

The advantage of the open-source nature of many of these analysis tools is that it allows subsequent researchers to build upon previous work for their own applications. One such example of this is the open-source Python package TEMUL toolkit, which builds upon the Hyperspy[96] and Atomap packages for quantification and visualization of STEM data[97]. Within the TEMUL toolkit, the TopoTEM module can be used to further analyze lattice positions extracted by Atomap. Several additional functionalities are introduced, including the ability to average polarization vectors over several unit cells, varying the vector color with polarization angle, and contour plots, as illustrated in Figure 4C[95].

With the improved user-friendliness of electron microscopy equipment and the availability of open-source software for image quantification, numerous opportunities arise for novel approaches to image analysis. Many properties of ferroic materials, such as relaxor ferroelectricity, result from short- to medium-range ordering of chemical composition or structural distortion[40,98]. One innovative approach to analyzing the interplay of local structure and chemistry and its spatial variation in a relaxor ferroelectric is to utilize methods commonly applied to Geographic Information Systems (GIS). In this example, GIS analysis indicates a strong correlation between chemical and oxygen octahedral distortion ordering and a weak correlation between oxygen octahedral and tilt ordering[99]. Such analyses can provide insights into important correlations between different types of short-range order in piezoelectric materials and in structural materials such as high-entropy alloys.

4D-STEM data analysis

While 4D-STEM presents tremendous opportunities for characterizing piezoelectric materials at the microscale to atomic resolution, the technique also presents unique challenges related to the size and scope
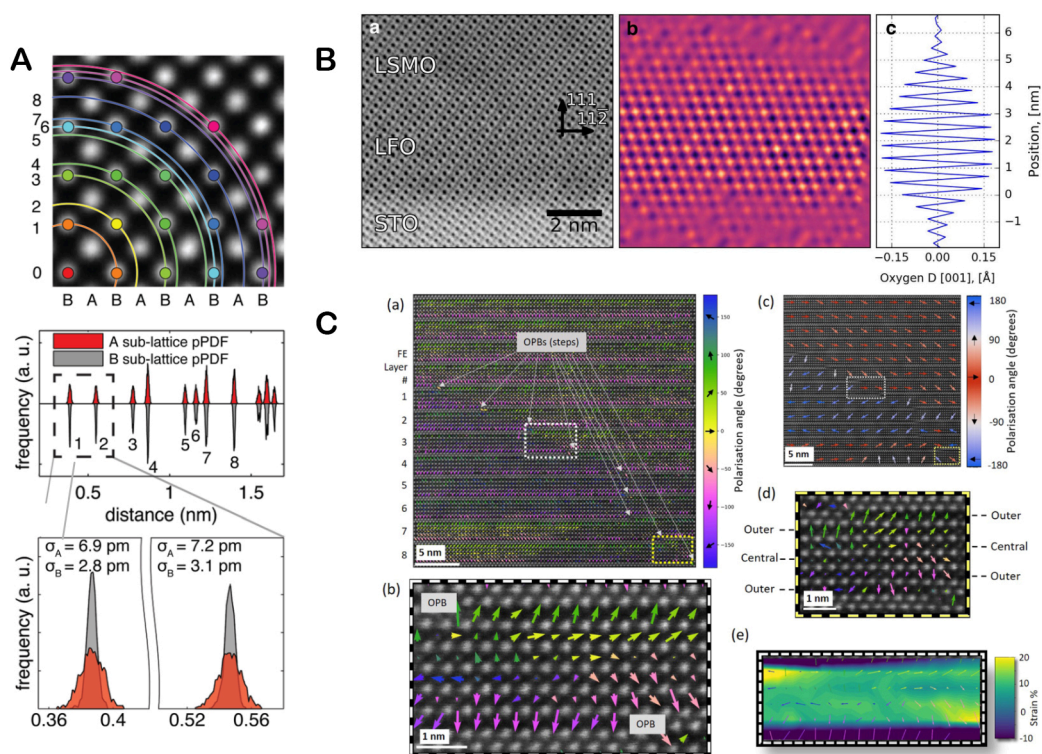
Figure 4. (A) Analyzing atom column positions to find the projected pair distribution functions of the A and B sublattices. Adapted with permission[87]. Copyright © 2015 AIP Publishing. (B) Utilizing Atomap to find the displacement of oxygen columns in the [001] direction from an ABF-STEM image. Adapted with permission[82]. Copyright © 2017 Springer. (C) Various polarization plots at domain walls for $Bi_6Ti_xFe_yMn_zO_{16}$ multiferroic thin films created with TopoTEM. Numerous plotting features, including angle-dependent vector colors, area-averaged polarization, and contour plots, are illustrated to highlight domain walls. Reprinted with permission[95]. Copyright © 2022 American Chemical Society.

of the datasets. For example, a 128 × 128 pixel scan, with each position containing a 256 × 256 pixel diffraction pattern, produces a dataset that is several gigabytes in size. Increasing the number of pixels in either the 2D images or the 2D diffraction patterns can further expand the size of a single data set to hundreds of gigabytes or even several terabytes[19]. Manually analyzing the vast quantity of data in even a small 4D-STEM data set is infeasible, making computational techniques critical for in-depth materials analysis. To facilitate material analysis with 4D-STEM, high computational power coupled with programmatic tools is essential. In the following section, we will outline some of the software available for analyzing 4D-STEM data.

To maximize the value of obtaining large 4D-STEM datasets, it is crucial to have tools available that enable researchers of various skill levels and backgrounds to extract meaningful data from these experiments. For instance, strain mapping requires measuring the spacing of diffraction disks, which is impractical to perform by manually identifying the disks and measuring their spacing. As discussed in previous sections, open-source software provides the best opportunity for widespread applications of these useful techniques.

One of the most valuable software packages for analyzing 4D-STEM data is py4DSTEM, an open-source Python package that facilitates data visualization and analysis[100,101]. A good starting point for 4D-STEM data analysis is multimodal imaging, which allows for the observation of various imaging modes (e.g., BF, HAADF, DPC, *etc.*) from a single dataset. In this context, py4DSTEM employs a graphical user interface that can generate images by selecting the diffraction information included in the image via a "virtual

detector". Conversely, it allows the selection of a region of interest in the image to produce a Bragg Vector Map (BVM), which collapses the diffraction information into a single image[100,101]. This information can be collected at various points in the image for further analysis, such as orientation mapping and strain mapping. Furthermore, py4DSTEM has built-in functionalities that enable users to locate diffraction disks and make quantitative measurements for parameters such as strain and polarization. This capability ensures that measurements can be standardized and repeated across a variety of datasets, facilitating repeatable analysis.

Although programs, such as py4DSTEM, provide a strong foundation for analyzing 4D-STEM datasets, there are cases where researchers need to develop custom tools for their specific applications. Automated analysis is the most practical approach for such analyses, but often, custom solutions need to be built. For instance, some datasets may contain noisy and complex features that require filtering and fitting algorithms. One recently introduced program is AutoDisk, a Python-based code that performs automated diffraction processing for strain mapping. Variations in diffraction patterns can arise due to various factors, including thickness gradients and low probe currents for beam-sensitive materials, which can complicate automated analysis. AutoDisk addresses these variations by utilizing cross-correlations, blob detection, edge refinements, and lattice fitting to identify diffraction disks[102]. Once identified, this diffraction information can be used for various analyses, including characterizing phase, symmetry, and orientation. While there are many ways to analyze data, unique solutions may be necessary for analyzing specific datasets. There are numerous code repositories available for 4D-STEM data analysis, including py4DSTEM, HyperSpy, pyXem, LiberTEM, and Pycroscopy, which can serve as a basis for custom analysis[19].

SUMMARY AND OUTLOOK

In conclusion, electron microscopy is a dynamic and continuously advancing technique with immense potential for the analysis of ferroic and other functional materials. Ferroic materials exhibit a wide range of unique properties that can be utilized in countless applications. These properties stem from chemical and structural inhomogeneities that occur at the atomic scale.

S/TEM offers a distinct advantage in probing these features in both real space and reciprocal space through electron diffraction measurements. Recent advancements in electron microscopy technology have improved the usability and enabled unprecedented resolution of these instruments. To fully harness the potential of S/TEM in the development of advanced materials, it is crucial to make data collection and analysis widely accessible to researchers. This accessibility will foster further exploration and utilization of S/TEM in material characterization. The field holds incredible potential, which can be further realized through ongoing advancements and the collaboration of researchers from various disciplines.

(1) Instrumentation availability and data analysis tools: STEM and TEM play a crucial role in the study of piezoelectric and other functional materials. While state-of-the-art instruments are not immediately available to all researchers, instruments are often accessible to external researchers at universities, national laboratories, and in industry. There are two aspects to make TEM and STEM available to more researchers:

a. Data collection: Modern S/TEM user interfaces are equipped with programmatic capabilities, enabling users to develop workflows to streamline data collection. S/TEMs can readily interface with Python code or support the user of custom scripts such as Gatan's Digital Micrograph. It is essential to promote the open-source nature of these programs so they can be utilized by researchers from various backgrounds. Simplifying data collection will allow researchers to allocate more time for analysis and characterization.

b. Data analysis: With the advancement in S/TEM instrumentation, the alignment and probe-correction processes have become more streamlined, allowing researchers to dedicate more time to data processing. Whether it involves HAADF or 4D-STEM imaging, data analysis remains a critical step in extracting meaningful information from images. To promote the widespread accessibility of advanced electron microscopy and analysis, it is crucial to make these tools readily available to all researchers. When publishing data, it is important to provide the associated analysis tools to ensure the repeatability of measurements and enable further development. By making analysis tools readily available, researchers can reproduce and validate the results obtained by their peers. Moreover, it allows for the exploration of alternative analysis techniques and the advancement of the field. This open sharing of analysis tools fosters collaboration, facilitates scientific progress, and maximizes the value of the obtained data.

(2) Development of 4D-STEM: Direct electron and pixelated detectors have opened new possibilities for advanced electron microscopy. Despite significant advancements in the last decade, there are many opportunities for additional applications. This includes the use of 4D-STEM with *in-situ* microscopy to characterize dynamic processes in materials. Although the data collection process for 4D-STEM is typically slower than with conventional detectors, the technique allows in-depth characterization of features such as domains and strain fields. The stability of modern *in-situ* systems makes this a promising direction for functional materials research.

Overall, electron microscopy holds tremendous potential for advanced characterization in the study of ferroic and the broader category of functional materials. The continuous development of instrumentation and data processing methods has allowed for deep insights into the characterization of advanced materials, which are crucial for understanding the intricate relationships between structure and properties. While there have been significant advancements in the field, it is important to recognize that there is still work to be done. Further efforts are needed to expand the scope of characterization techniques and enhance the accessibility of electron microscopy to researchers from diverse backgrounds. This includes developing new imaging modalities, improving data analysis tools, and making these resources widely available. By pushing the boundaries of electron microscopy, we can unlock discoveries and gain a deeper understanding of piezoelectric materials. Continuous advancements and the collaborative efforts of scientists across disciplines will play a crucial role in expanding the capabilities and accessibility of electron microscopy for the benefit of scientific research and technological advancements.

DECLARATIONS

Authors' contributions
Conceptual design and manuscript draft: Cabral MJ
Manuscript revision and project supervision: Chen Z, Liao X

Availability of data and materials
Not applicable.

Conflicts of interest

All authors declared that there are no conflicts of interest.

Ethical approval and consent to participate

Not applicable.

Consent for publication

Not applicable.

Copyright

© The Author(s) 2023.

REFERENCES

1.   Covaci C, Gontean A. Piezoelectric energy harvesting solutions: a review. *Sensors* 2020;20:3512. DOI PubMed PMC
2.   Sezer N, Koç M. A comprehensive review on the state-of-the-art of piezoelectric energy harvesting. *Nano Energy* 2021;80:105567. DOI
3.   Shung KK, Cannata JM, Zhou QF. Piezoelectric materials for high frequency medical imaging applications: a review. *J Electroceram* 2007;19:141-7. DOI
4.   Sekhar MC, Veena E, Kumar NS, Naidu KCB, Mallikarjuna A, Basha DB. A review on piezoelectric materials and their applications. *Cryst Res Technol* 2023;58:2200130. DOI
5.   Iqbal M, Nauman MM, Khan FU, et al. Vibration-based piezoelectric, electromagnetic, and hybrid energy harvesters for microsystems applications: a contributed review. *Int J Energy Res* 2021;45:65-102. DOI
6.   Li F, Lin D, Chen Z, et al. Ultrahigh piezoelectricity in ferroelectric ceramics by design. *Nat Mater* 2018;17:349-54. DOI
7.   Li F, Cabral MJ, Xu B, et al. Giant piezoelectricity of Sm-doped $Pb(Mg_{1/3}Nb_{2/3})O_3$-$PbTiO_3$ single crystals. *Science* 2019;364:264-8. DOI
8.   Zhang S. High entropy design: a new pathway to promote the piezoelectricity and dielectric energy storage in perovskite oxides. *Microstructures* 2022;3:2023003. DOI
9.   Batson PE, Dellby N, Krivanek OL. Sub-angstrom resolution using aberration corrected electron optics. *Nature* 2002;418:617-20. DOI
10. Krivanek O, Dellby N, Lupini A. Towards sub-Å electron beams. *Ultramicroscopy* 1999;78:1-11. DOI
11. Hetherington C. Aberration correction for TEM. *Mater Today* 2004;7:50-5. DOI
12. Voyles PM, Muller DA, Grazul JL, Citrin PH, Gossmann HJ. Atomic-scale imaging of individual dopant atoms and clusters in highly n-type bulk Si. *Nature* 2002;416:826-9. DOI PubMed
13. Voyles PM, Grazul JL, Muller DA. Imaging individual atoms inside crystals with ADF-STEM. *Ultramicroscopy* 2003;96:251-73. DOI PubMed
14. Jiang Y, Chen Z, Han Y, et al. Electron ptychography of 2D materials to deep sub-ångström resolution. *Nature* 2018;559:343-9. DOI
15. Liu C, Cui J, Cheng Z, et al. Direct observation of oxygen atoms taking tetrahedral interstitial sites in medium-entropy body-centered-cubic solutions. *Adv Mater* 2023;35:e2209941. DOI
16. Close R, Chen Z, Shibata N, Findlay SD. Towards quantitative, atomic-resolution reconstruction of the electrostatic potential via differential phase contrast using electrons. *Ultramicroscopy* 2015;159 Pt 1:124-37. DOI PubMed
17. Krivanek OL, Lovejoy TC, Dellby N, et al. Vibrational spectroscopy in the electron microscope. *Nature* 2014;514:209-12. DOI
18. de la Mata M, Molina SI. STEM tools for semiconductor characterization: beyond high-resolution imaging. *Nanomaterials* 2022;12:337. DOI PubMed PMC
19. Ophus C. Four-dimensional scanning transmission electron microscopy (4D-STEM): from scanning nanodiffraction to ptychography and beyond. *Microsc Microanal* 2019;25:563-82. DOI PubMed
20. Lin Y, Zhou M, Tai X, Li H, Han X, Yu J. Analytical transmission electron microscopy for emerging advanced materials. *Matter* 2021;4:2309-39. DOI
21. Williams DB, Carter CB. Transmission electron microscopy. New York: Springer; 1996. DOI
22. Lebeau JM, Stemmer S. Experimental quantification of annular dark-field images in scanning transmission electron microscopy. *Ultramicroscopy* 2008;108:1653-8. DOI PubMed
23. LeBeau JM, Findlay SD, Allen LJ, Stemmer S. Quantitative atomic resolution scanning transmission electron microscopy. *Phys Rev Lett* 2008;100:206101. DOI PubMed
24. Muller DA, Nakagawa N, Ohtomo A, Grazul JL, Hwang HY. Atomic-scale imaging of nanoengineered oxygen vacancy profiles in $SrTiO_3$. *Nature* 2004;430:657-61. DOI PubMed
25. Fitting L, Thiel S, Schmehl A, Mannhart J, Muller DA. Subtleties in ADF imaging and spatially resolved EELS: a case study of low-angle twist boundaries in $SrTiO_3$. *Ultramicroscopy* 2006;106:1053-61. DOI PubMed

26.   Zhang W, Zhang X, Xu P, et al. Structure domains induced nonswitchable ferroelectric polarization in polar doubly cation-ordered perovskites. *Ceram Int* 2022;48:30853-8. DOI

27.   Campanini M, Erni R, Yang CH, Ramesh R, Rossell MD. Periodic giant polarization gradients in doped BiFeO$_3$ thin films. *Nano Lett* 2018;18:717-24. DOI PubMed

28.   Shur VY, Akhmatkhanov AR, Baturin IS. Micro- and nano-domain engineering in lithium niobate. *App Phys Rev* 2015;2:040604. DOI

29.   Okunishi E, Ishikawa I, Sawada H, Hosokawa F, Hori M, Kondo Y. Visualization of light elements at ultrahigh resolution by STEM annular bright field microscopy. *Microsc Microanal* 2009;15:164-5. DOI

30.   Findlay SD, Shibata N, Sawada H, et al. Robust atomic resolution imaging of light elements using scanning transmission electron microscopy. *Appl Phys Lett* 2009;95:191913. DOI

31.   Ge W, Beanland R, Alexe M, Ramasse Q, Sanchez AM. 180° head-to-head flat domain walls in single crystal BiFeO$_3$. *Microstructures* 2023;3:2023026. DOI

32.   Ishikawa R, Okunishi E, Sawada H, Kondo Y, Hosokawa F, Abe E. Direct imaging of hydrogen-atom columns in a crystal by annular bright-field electron microscopy. *Nat Mater* 2011;10:278-81. DOI

33.   Okunishi E, Sawada H, Kondo Y. Experimental study of annular bright field (ABF) imaging using aberration-corrected scanning transmission electron microscopy (STEM). *Micron* 2012;43:538-44. DOI

34.   Vogel A, Sarott MF, Campanini M, Trassin M, Rossell MD. Monitoring electrical biasing of Pb(Zr$_{0.2}$Ti$_{0.8}$)O$_3$ ferroelectric thin films in situ by DPC-stem imaging. *Materials* 2021;14:4749. DOI PubMed PMC

35.   Yücelen E, Lazić I, Bosch EGT. Phase contrast scanning transmission electron microscopy imaging of light and heavy atoms at the limit of contrast and resolution. *Sci Rep* 2018;8:2676. DOI PubMed PMC

36.   Rose H. Nonstandard imaging methods in electron microscopy. *Ultramicroscopy* 1977;2:251-67. DOI PubMed

37.   Chapman JN, Batson PE, Waddell EM, Ferrier RP. The direct determination of magnetic domain wall profiles by differential phase contrast electron microscopy. *Ultramicroscopy* 1978;3:203-13. DOI

38.   Shibata N, Findlay SD, Kohno Y, Sawada H, Kondo Y, Ikuhara Y. Differential phase-contrast microscopy at atomic resolution. *Nat Phys* 2012;8:611-5. DOI

39.   Lazić I, Bosch EGT, Lazar S. Phase contrast STEM for thin samples: integrated differential phase contrast. *Ultramicroscopy* 2016;160:265-80. DOI PubMed

40.   Kumar A, Baker JN, Bowes PC, et al. Atomic-resolution electron microscopy of nanoscale local structure in lead-based relaxor ferroelectrics. *Nat Mater* 2021;20:62-7. DOI

41.   Pennycook TJ, Lupini AR, Yang H, Murfitt MF, Jones L, Nellist PD. Efficient phase contrast imaging in STEM using a pixelated detector. Part 1: experimental demonstration at atomic resolution. *Ultramicroscopy* 2015;151:160-7. DOI PubMed

42.   Yang H, Pennycook TJ, Nellist PD. Efficient phase contrast imaging in STEM using a pixelated detector. Part II: optimisation of imaging conditions. *Ultramicroscopy* 2015;151:232-9. DOI PubMed

43.   Maclaren I, Macgregor TA, Allen CS, Kirkland AI. Detectors - the ongoing revolution in scanning transmission electron microscopy and why this important to material characterization. *APL Mater* 2020;8:110901. DOI

44.   Tate MW, Purohit P, Chamberlain D, et al. High dynamic range pixel array detector for scanning transmission electron microscopy. *Microsc Microanal* 2016;22:237-49. DOI

45.   Chen Z, Jiang Y, Shao YT, et al. Electron ptychography achieves atomic-resolution limits set by lattice vibrations. *Science* 2021;372:826-31. DOI

46.   Lozano JG, Martinez GT, Jin L, Nellist PD, Bruce PG. Low-dose aberration-free imaging of Li-rich cathode materials at various states of charge using electron ptychography. *Nano Lett* 2018;18:6850-5. DOI PubMed

47.   Chen Z, Odstrcil M, Jiang Y, et al. Mixed-state electron ptychography enables sub-Angstrom resolution imaging with picometer precision at low dose. *Nat Commun* 2020;11:2994. DOI PubMed PMC

48.   Zeltmann SE, Müller A, Bustillo KC, et al. Patterned probes for high precision 4D-STEM bragg measurements. *Ultramicroscopy* 2020;209:112890. DOI

49.   Mahr C, Müller-Caspary K, Grieb T, Krause FF, Schowalter M, Rosenauer A. Accurate measurement of strain at interfaces in 4D-STEM: a comparison of various methods. *Ultramicroscopy* 2021;221:113196. DOI PubMed

50.   Tsuda K, Yasuhara A, Tanaka M. Two-dimensional mapping of polarizations of rhombohedral nanostructures in the tetragonal phase of BaTiO$_3$ by the combined use of the scanning transmission electron microscopy and convergent-beam electron diffraction methods. *Appl Phys Lett* 2013;103:082908. DOI

51.   Mun J, Peng W, Roh CJ, et al. In situ cryogenic HAADF-STEM observation of spontaneous transition of ferroelectric polarization domain structures at low temperatures. *Nano Lett* 2021;21:8679-86. DOI

52.   Zheng H, Zhu Y. Perspectives on in situ electron microscopy. *Ultramicroscopy* 2017;180:188-96. DOI

53.   Ross FM. Opportunities and challenges in liquid cell electron microscopy. *Science* 2015;350:aaa9886. DOI PubMed

54.   Schneider NM, Norton MM, Mendel BJ, Grogan JM, Ross FM, Bau HH. Electron-water interactions and implications for liquid cell electron microscopy. *J Phys Chem C* 2014;118:22373-82. DOI

55.   Nukala P, Ahmadi M, Antoja-lleonart J, et al. *In situ* heating studies on temperature-induced phase transitions in epitaxial Hf$_{0.5}$Zr$_{0.5}$O$_2$/La$_{0.67}$Sr$_{0.33}$MnO$_3$ heterostructures. *Appl Phys Lett* 2021;118:062901. DOI

56.   Xu W, Bowes PC, Grimley ED, Irving DL, Lebeau JM. *In-situ* real-space imaging of single crystal surface reconstructions via

electron microscopy. *Appl Phys Lett* 2016;109:201601. DOI

57.   Zhu Y, Wang S, Li B, et al. Twist-to-untwist evolution and cation polarization behavior of hybrid halide perovskite nanoplatelets revealed by cryogenic transmission electron microscopy. *J Phys Chem Lett* 2021;12:12187-95. DOI

58.   Chen Z, Wang X, Ringer SP, Liao X. Manipulation of nanoscale domain switching using an electron beam with omnidirectional electric field distribution. *Phys Rev Lett* 2016;117:027601. DOI

59.   Chen Z, Li F, Huang Q, et al. Giant tuning of ferroelectricity in single crystals by thickness engineering. *Sci Adv* 2020;6:eabc7156. DOI PubMed PMC

60.   Chen Z, Huang Q, Wang F, Ringer SP, Luo H, Liao X. Stress-induced reversible and irreversible ferroelectric domain switching. *Appl Phys Lett* 2018;112:152901. DOI

61.   Chen Z, Hong L, Wang F, et al. Facilitation of ferroelectric switching via mechanical manipulation of hierarchical nanoscale domain structures. *Phys Rev Lett* 2017;118:017601. DOI

62.   Huang Q, Yang J, Chen Z, et al. Formation of head/tail-to-body charged domain walls by mechanical stress. *ACS Appl Mater Interfaces* 2023;15:2313-8. DOI

63.   Taheri ML, Stach EA, Arslan I, et al. Current status and future directions for in situ transmission electron microscopy. *Ultramicroscopy* 2016;170:86-95. DOI PubMed PMC

64.   Fan Z, Zhang L, Baumann D, et al. In situ transmission electron microscopy for energy materials and devices. *Adv Mater* 2019;31:e1900608. DOI

65.   Deng Y, Zhang R, Pekin TC, et al. Functional materials under stress: in situ TEM observations of structural evolution. *Adv Mater* 2020;32:e1906105. DOI

66.   Muller DA, Kirkland EJ, Thomas MG, Grazul JL, Fitting L, Weyland M. Room design for high-performance electron microscopy. *Ultramicroscopy* 2006;106:1033-40. DOI PubMed

67.   Ophus C, Ciston J, Nelson CT. Correcting nonlinear drift distortion of scanning probe and scanning transmission electron microscopies from image pairs with orthogonal scan directions. *Ultramicroscopy* 2016;162:1-9. DOI PubMed

68.   Jones L, Nellist PD. Identifying and correcting scan noise and drift in the scanning transmission electron microscope. *Microsc Microanal* 2013;19:1050-60. DOI PubMed

69.   Schnedler M, Weidlich PH, Portz V, Weber D, Dunin-Borkowski RE, Ebert P. Correction of nonlinear lateral distortions of scanning probe microscopy images. *Ultramicroscopy* 2014;136:86-90. DOI PubMed

70.   Berkels B, Binev P, Blom DA, Dahmen W, Sharpley RC, Vogt T. Optimized imaging using non-rigid registration. *Ultramicroscopy* 2014;138:46-56. DOI PubMed

71.   Berkels B, Liebscher CH. Joint non-rigid image registration and reconstruction for quantitative atomic resolution scanning transmission electron microscopy. *Ultramicroscopy* 2019;198:49-57. DOI PubMed

72.   Jones L, Yang H, Pennycook TJ, et al. Smart align - a new tool for robust non-rigid registration of scanning microscope data. *Adv Struct Chem Imaging* 2015;1:8. DOI

73.   Ihara S, Saito H, Yoshinaga M, Avala L, Murayama M. Deep learning-based noise filtering toward millisecond order imaging by using scanning transmission electron microscopy. *Sci Rep* 2022;12:13462. DOI PubMed PMC

74.   Sang X, LeBeau JM. Revolving scanning transmission electron microscopy: correcting sample drift distortion without prior knowledge. *Ultramicroscopy* 2014;138:28-35. DOI PubMed

75.   Dycus JH, Harris JS, Sang X, et al. Accurate nanoscale crystallography in real-space using scanning transmission electron microscopy. *Microsc Microanal* 2015;21:946-52. DOI

76.   Borisevich A, Ovchinnikov OS, Chang HJ, et al. Mapping octahedral tilts and polarization across a domain wall in $BiFeO_3$ from Z-contrast scanning transmission electron microscopy image atomic column shape analysis. *ACS Nano* 2010;4:6071-9. DOI

77.   Zuo JM, Shah AB, Kim H, Meng Y, Gao W, Rouviére JL. Lattice and strain analysis of atomic resolution Z-contrast images based on template matching. *Ultramicroscopy* 2014;136:50-60. DOI PubMed

78.   Kirkland EJ, Loane RF, Silcox J. Simulation of annular dark field stem images using a modified multislice method. *Ultramicroscopy* 1987;23:77-96. DOI

79.   Barthel J. Dr. Probe: A software for high-resolution STEM image simulation. *Ultramicroscopy* 2018;193:1-11. DOI PubMed

80.   Lazić I, Bosch EGT. Chapter three - analytical review of direct stem imaging techniques for thin samples. *Adv Imaging Electron Phys* 2017;199:75-184. DOI

81.   Sang X, Oni AA, LeBeau JM. Atom column indexing: atomic resolution image analysis through a matrix representation. *Microsc Microanal* 2014;20:1764-71. DOI PubMed

82.   Nord M, Vullum PE, MacLaren I, Tybell T, Holmestad R. Atomap: a new software tool for the automated analysis of atomic resolution images using two-dimensional Gaussian fitting. *Adv Struct Chem Imaging* 2017;3:9. DOI PubMed PMC

83.   Backer A, van den Bos KHW, Van den Broek W, Sijbers J, Van Aert S. StatSTEM: an efficient approach for accurate and precise model-based quantification of atomic resolution electron microscopy images. *Ultramicroscopy* 2016;171:104-16. DOI PubMed

84.   Zhang Q, Zhang LY, Jin CH, Wang YM, Lin F. CalAtom: a software for quantitatively analysing atomic columns in a transmission electron microscope image. *Ultramicroscopy* 2019;202:114-20. DOI

85.   Wang Y, Salzberger U, Sigle W, Eren Suyolcu Y, van Aken PA. Oxygen octahedra picker: a software tool to extract quantitative information from STEM images. *Ultramicroscopy* 2016;168:46-52. DOI

86.   Du H. DMPFIT: a tool for atomic-scale metrology via nonlinear least-squares fitting of peaks in atomic-resolution TEM images.

Nanomanuf Metrol 2022;5:101-11. DOI

87. Sang X, Grimley ED, Niu C, Irving DL, Lebeau JM. Direct observation of charge mediated lattice distortions in complex oxide solid solutions. *Appl Phys Lett* 2015;106:061913. DOI

88. Oni AA, Sang X, Raju SV, et al. Large area strain analysis using scanning transmission electron microscopy across multiple images. *Appl Phys Lett* 2015;106:011601. DOI

89. Hytch MJH, Snoeck E, Kilaas R. Quantitative measurement of displacement and strain fields from HREM micrographs. *Ultramicroscopy* 1998;74:131-46. DOI

90. Rouviere J, Béché A, Martin Y, Denneulin T, Cooper D. Improved strain precision with high spatial resolution using nanobeam precession electron diffraction. *Appl Phys Lett* 2013;103:241913. DOI

91. Zhao L, Liu Q, Gao J, Zhang S, Li JF. Lead-free antiferroelectric silver niobate tantalate with high energy storage performance. *Adv Mater* 2017;29:1701824. DOI

92. Jeong IK, Darling TW, Lee JK, et al. Direct observation of the formation of polar nanoregions in $Pb(Mg_{1/3}Nb_{2/3})O_3$ using neutron pair distribution function analysis. *Phys Rev Lett* 2005;94:147602. DOI

93. Wu H, Zhang Y, Wu J, Wang J, Pennycook SJ. Microstructural origins of high piezoelectric performance: a pathway to practical lead-free materials. *Adv Funct Mater* 2019;29:1902911. DOI

94. Fiebig M. Revival of the magnetoelectric effect. *J Phys D Appl Phys* 2005;38:R123. DOI

95. Moore K, O'Connell EN, Griffin SM, et al. Charged domain wall and polar vortex topologies in a room-temperature magnetoelectric multiferroic thin film. *ACS Appl Mater Interfaces* 2022;14:5525-36. DOI PubMed PMC

96. de la Peña F, Prestat E, Fauske VT, et al. Hyperspy/hyperspy: release v1.7.3. 2022. DOI

97. O'Connell EN, Moore K, McFall E, et al. TopoTEM: a python package for quantifying and visualizing scanning transmission electron microscopy data of polar topologies. *Microsc Microanal* 2022;28:1444-52. DOI

98. Cabral MJ, Zhang S, Dickey EC, Lebeau JM. Gradient chemical order in the relaxor $Pb(Mg_{1/3}Nb_{2/3})O_3$. *Appl Phys Lett* 2018;112:082901. DOI

99. Xu M, Kumar A, LeBeau JM. Correlating local chemical and structural order using geographic information systems-based spatial statistics. *Ultramicroscopy* 2023;243:113642. DOI PubMed

100. Savitzky BH, Zeltmann SE, Hughes LA, et al. py4DSTEM: a software package for four-dimensional scanning transmission electron microscopy data analysis. *Microsc Microanal* 2021;27:712-43. DOI

101. Savitzky BH, Hughes L, Bustillo KC, et al. py4DSTEM: open source software for 4D-STEM data analysis. *Microsc Microanal* 2019;25:124-5. DOI

102. Wang S, Eldred TB, Smith JG, Gao W. AutoDisk: automated diffraction processing and strain mapping in 4D-STEM. *Ultramicroscopy* 2022;236:113513. DOI PubMed